


RESEARCH

Open Access



Contribution of advanced neuro-imaging (MR diffusion, perfusion and proton spectroscopy) in differentiation between low grade gliomas GII and MR morphologically similar non neoplastic lesions

Mohamed Saied Abdelgawad^{1*} , Mohamed Hamdy Kaye², Mohamed Ihab Samy Reda², Eman Abdelzahr³, Ahmed Hafez Farhoud⁴ and Nermeen Elsebaie²

Abstract

Background: Non-neoplastic brain lesions can be misdiagnosed as low-grade gliomas. Conventional magnetic resonance (MR) imaging may be non-specific. Additional imaging modalities such as spectroscopy (MRS), perfusion and diffusion imaging aid in diagnosis of such lesions. However, contradictory and overlapping results are still present. Hence, our purpose was to evaluate the role of advanced neuro-imaging in differentiation between low-grade gliomas (WHO grade II) and MR morphologically similar non-neoplastic lesions and to prove which modality has the most accurate results in differentiation.

Results: All patients were classified into two main groups: patients with low-grade glioma ($n = 12$; mean age, 38.8 ± 16 ; 8 males) and patients with non-neoplastic lesions ($n = 27$; mean age, 36.6 ± 15 ; 19 males) based on the histopathological and clinical–radiological diagnosis. Using ROC curve analysis, a threshold value of 0.93 for rCBV (AUC = 0.875, PPV = 92%, NPV = 71.4%) and a threshold value of 2.5 for Cho/NAA (AUC = 0.829, PPV = 92%, NPV = 71.4%) had 85.2% sensitivity and 83.3% specificity for predicting neoplastic lesions. The area under the curve (AUC) of ROC analysis was good for relative cerebral blood volume (rCBV) and Cho/NAA ratios (> 0.80) and fair for Cho/Cr and NAA/Cr ratios (0.70–0.80). When the rCBV measurements were combined with MRS ratios, significant improvement was observed in the area under the curve (AUC) (0.969) with improved diagnostic accuracy (89.7%) and sensitivity (88.9%).

Conclusions: Evaluation of rCBV and metabolite ratios at MRS, particularly Cho/NAA ratio, may be helpful in differentiating low-grade gliomas from non-neoplastic lesions. The combination of dynamic susceptibility contrast (DSC) perfusion and MRS can significantly improve the diagnostic accuracy and can help avoiding the need for an invasive biopsy.

Keywords: Low grade glioma, Non-neoplastic lesions, Magnetic resonance imaging, Diffusion weighted images, Perfusion weighted images, Proton magnetic resonance spectroscopy

Background

Differentiation between neoplastic and non-neoplastic intra-axial brain lesions is not an easy task using conventional magnetic resonance (MR) imaging and

*Correspondence: mselgawad@yahoo.com

¹ Radiology Department, National Liver Institute, Menoufia University, Shibin Al Kawm, Egypt

Full list of author information is available at the end of the article

requires further work up. Currently, the role of imaging exceeded anatomic analysis for reaching diagnosis by additional physiological and metabolic information as well [1].

Several types of non-neoplastic brain lesions such as tumefactive demyelinating lesions, sub-acute vascular insults and intra axial brain infection can be potentially misinterpreted as brain tumors. Appearance of these lesions in the conventional MR imaging may be nonspecific and even mimics the appearance of intra axial brain tumors such as low-grade gliomas, the use of a contrast agent may not also add a significant value for proper differentiation between these types of lesions because any pathologic process interfering with the blood–brain barrier integrity can result in enhancement on MR imaging [2].

There is a need for advanced neuro-imaging modalities to solve this problem. The most commonly used advanced MR imaging modalities, such as perfusion and diffusion-weighted imaging as well as spectroscopy add important information about cellular integrity and metabolism that help in the diagnosis of these unknown brain lesions. However, they are still under investigation [3], since limited data are available on their use particularly in the differentiation between non-neoplastic lesions from low-grade tumors [4].

The rule is that advanced neuroimaging combines both the spatial localization capabilities of MR imaging with the biochemical and functional information from tissues which has proved to be useful in discriminating between the different tumor types as well as discriminating between tumors and pseudo-tumors by depicting metabolic changes reflective of cellular density, anaplasia and mitotic index [4, 5].

Diffusion-weighted imaging (DWI) measures the degree of diffusion of water molecules in vivo (within the biologic tissues). Diffusion within the tumor is a direct reflection of the degree of cellular density within because intact cells form a barrier to water diffusion resulting in restricted diffusion measured by apparent diffusion coefficient (ADC) maps [6]. In normal adult brain, the ADC values in the gray matter range between 0.8 and $1.1 \times 10^{-3} \text{ mm}^2/\text{s}$, and those in the white matter range between 0.6 and $0.9 \times 10^{-3} \text{ mm}^2/\text{s}$ [7].

Perfusion MR imaging is an indirect marker for blood supply in the biologic tissue such as tumors and a sensitive tool for detection of neo-vascularity. Post-processing of the acquired data aid for calculation of physiologic parameters such as cerebral blood flow, cerebral blood volume (CBV), mean transit time, and time to peak. CBV measurements are commonly made relative to the contralateral normal appearing white matter (CBV in the lesion/CBV in the contralateral normal appearing white

matter). Tumors usually have higher relative CBV (rCBV) values than non-neoplastic lesions [8, 9].

MR spectroscopy (MRS) obtains metabolic information from biologic tissue noninvasively. Within a defined region of interest and with adequate water suppression, signals could be detected from chemical nuclei within the tissue; the most commonly used nuclei are protons and phosphors [10, 11]. The frequently assessed metabolites at MRS include *N*-acetyl aspartate (NAA) assigned at 2.02 ppm, creatine (Cr) assigned at 3.02 ppm, choline (Cho) assigned at 3.22 ppm. Peak of lactate (Lac) is hardly visualized in the normal brain and is assigned at 1.33 ppm as a doublet. No lipid peaks are detected in normal brain tissue. Tumors, with special emphasis on low grade gliomas, would display decrease of NAA and creatine peaks and increase of choline, lipids and lactate peaks, in contrast to non-neoplastic lesions which are characterized by maintained NAA and creatine peaks and increase of choline and lactate peaks [11].

Combination of the data obtained from both advanced and conventional MR imaging enhance the radiologist's ability to specify the vague and non-classical intra-axial lesions with a higher degree of confidence [12, 13]. The major diagnostic challenge is to reliably, noninvasively, and promptly discriminate low grade neoplastic lesions from non-neoplastic lesions to avoid biopsy and follow-up imaging studies [14, 15].

Hence, our purpose was to evaluate the role of advanced neuro-imaging in differentiation between low-grade gliomas (WHO grade II) and MR morphologically similar non neoplastic lesions and to prove which modality has the most accurate results in differentiation.

Methods

Data collection

In this prospective study, patients were included if there was evidence of mass like lesion at conventional MRI of the brain. The final diagnosis was made from either histopathologic result after surgical resection or biopsy or clinical–radiologic diagnosis. For clinical–radiologic diagnosis, a follow-up MRI after 1 year was used as the reference standard. The following exclusion criteria were applied: patients younger than 16 years of age; patients who had undergone surgery before MRI examination, patients without complete MRI protocol and patients with non-diagnostic DWI, perfusion or MRS sequences due to motion artifacts. Hence, over the course of two years starting December 2013 till December 2015, total patients' count was 39 adult patients (27 males and 12 females), their age ranged from 16 to 65 years with a mean of $37.6 \text{ years} \pm 17.3$. Informed consent was obtained from all patients and the study was approved by the Ethics Committee of our institution.

Imaging techniques and analysis

MR imaging was performed using Siemens Avanto 1.5 MR system with a standard head coil. Each study consisted of axial and coronal T2-weighted turbo spin echo (T2 TSE) utilizing repetition time (TR) of 3000 ms, an echo time (TE) of 120 ms, axial fluid-attenuated inversion recovery (FLAIR) (TR/TE, 8000/138, time of inversion (TI)=2000 ms), pre-contrast axial, coronal and sagittal T1-weighted spin echo (T1 SE) (550/15), and post contrast conventional axial, sagittal and coronal T1 spin echo (550/15), with 3 mm slice thickness, 0.3 mm gap, 256 × 256 acquisition matrix, and 180 mm field of view (FOV).

Diffusion analysis

DWI was performed in the axial plane, using a T2-weighted, echo-planar spin-echo sequence EPI with the following parameters: TR=3400 ms, TE=100 ms, 192 × 192 acquisition matrix, 5 mm slice thickness, 0.3 mm gap and b -value=0, 500, 1000 s/mm². The minimum ADC value was measured in the lesion core using a region of interest (ROI) while preferably avoiding cystic and necrotic areas. Standard mean ADC values were calculated automatically and expressed in 10⁻³ mm²/s. ROIs were also drawn on the contralateral normal-appearing brain parenchyma as a control [16].

Perfusion analysis

The perfusion weighted imaging (PWI) protocol was performed with a T2-weighted, echo-planar, spin-echo sequence (EPI) using the following parameters: TR=1480, TE=30, 128 × 128 acquisition matrix, 5 mm section thickness, no gap, and 50 scans. Gadopentetate dimeglumine contrast medium was injected at a dose of 0.1 mmol/kg using a power injector at a flow rate of 5 ml/s followed by a saline bolus (20 ml). Nineteen images per second were then acquired. Data processing was performed by using an Syngo Neuro Perfusion Evaluation as the analytic program. As the color maps of cerebral blood volume were generated, the maximum CBV in the lesion was calculated by placing the ROI in the solid areas showing the highest color intensity. Data were then compared with those of the ipsilateral or contralateral normal-appearing white matter to measure the relative CBV ($rCBV = CBV$ of the lesion/ CBV of normal appearing white matter). CBV of the normal appearing white matter is considered as a reference, lesions with $rCBV$ less than that of the whiter matter is considered hypo perfuse, and above is considered hyper perfused.

Spectroscopy analysis

Multi-voxel two-dimensional chemical shift imaging (2D CSI) was performed with an echo time of intermediate TE (135 ms) (TR 1,500 ms, FOV 160 mm, acquisition time 7 min 34 s) to evaluate the levels of choline (Cho) 3.36–3.21 ppm, creatine (Cr) 3.15–3.0 ppm, *N*-acetyl aspartate (NAA) 2.18–2.01 ppm, lactate 1.35 ppm and lipids 1.33–0.9 ppm using a point resolved spectroscopy (PRESS) sequences. The volume of interest size and position were determined by examining the MR images in all three dimensions (sagittal, coronal and transverse planes), the aim is to include the largest portion of the lesion, peri-focal area together with normal contra-lateral brain within the region of interest (only with assessment by multi-voxel 2D CSI) as much as we can and to exclude subcutaneous fat and regions with large variations in magnetic susceptibility. Appropriate automatic shimming achieved by using 4–8-Hz line width, 1-kHz spectral width, Water suppression using chemical shift selective saturation technique (CHESS) were done and the automated software developed by the manufacture spectroscopic data (Syngo neuro spectroscopy evaluation). The metabolite ratios: Cho/Cr, Cho/NAA, NAA/Cr and NAA/Cho were calculated by dividing the metabolite integral values in the same spectrum and it was done automatically by the work station software.

Pathological analysis

Seventeen cases could be confirmed by pathology. Routinely processed paraffin-embedded tissues were cut and stained with the conventional hematoxylin and eosin stain and reticulin stain. Immunohistochemical analysis was performed for CD20, CD3, pancytokeratin and S-100. Both the primary antibody and the detection kit were purchased from Lab Vision Corporation (Neo Markers, USA). Immunohistochemical staining was performed using an avidin-biotinylated immunoperoxidase methodology.

Follow-up MRI

Follow-up MRI was done for the non-biopsied cases including conventional MRI studies and advanced neuro-imaging for confirmation of the preliminary diagnosis. Patients were considered to have non-neoplastic process if they had regressive or vanishing lesions after treatment documented on MRI at 1 year follow-up.

Statistical analysis

Statistical analysis of the data was carried out using SPSS version 18. Descriptive statistical analysis was presented as counts and percentages for categorical

variables and as mean and standard deviation for continuous variables. For comparison of the quantitative variables between the low-grade glioma and non-neoplastic groups, we applied the Student-*t* test. A *P* value < 0.05 was considered statistically significant. We used a receiver operating characteristic analysis curve (ROC) to decide the cutoff between low-grade gliomas and non-neoplastic lesions. We then calculated the accuracy, sensitivity, specificity, positive predictive values (PPV) and negative predictive values (NPV) associated with these cutoff points (all values are presented as %).

Results

All patients were classified into two main groups: patients with low-grade glioma (*n* = 12; mean age, 38.8 ± 16; 8 males) and patients with non-neoplastic lesions (*n* = 27; mean age, 36.6 ± 15; 19 males) based on the histopathological and clinical–radiological diagnosis. All patients with low-grade brain tumors were confirmed on neuropathologic examination; the diagnosis was diffuse astrocytoma WHO grade II. In the 27 patients with non-neoplastic lesions, 5 patients were confirmed on neuropathologic examination (2 with pyogenic abscess, 2 with tuberculoma, 1 cavernoma) and in 22 patients, final diagnosis was achieved clinico-radiologically. Clinical–radiological diagnosis was determined by a combination of clinical history, cerebrospinal fluid analysis and post-treatment follow-up in patients with tumefactive demyelination (*n* = 7), ischemic infarction (*n* = 4), cavernoma (*n* = 3), encephalitis (*n* = 3), tuberculoma (*n* = 2), vasculitis (*n* = 2) and focal cortical dysplasia (*n* = 1).

Comparison of ADC, rCBV values and metabolite ratios between low-grade gliomas and non-neoplastic lesions

In DWI, ADC values in low-grade gliomas ranged from 0.42 to 2.2×10^{-3} mm²/s with a mean value of $1.2 \pm 0.5 \times 10^{-3}$ mm²/s. In non-neoplastic lesions, ADC values ranged from 0.53 to 1.5×10^{-3} mm²/s with a mean value of $1.13 \pm 0.32 \times 10^{-3}$ mm²/s, with no statistically significant difference between both groups (*P* = 0.74). In MR perfusion, rCBV was significantly higher in low-grade gliomas than non-neoplastic lesions (mean, 1.27 ± 0.45 vs. 0.75 ± 0.22 ; *P* < 0.001).

In MRS, Cho/NAA ratio was significantly higher in low-grade gliomas as compared to non-neoplastic lesions (mean, 3.34 ± 1.53 vs. 1.5 ± 1.6 ; *P* < 0.002). Cho/Cr was significantly higher in low-grade gliomas than in non-neoplastic lesions (2.14 ± 0.7 vs. 1.65 ± 1.1 ; *P* = 0.045). NAA/Cr ratio was significantly lower in low-grade gliomas (0.62 ± 0.27 vs. 1.46 ± 1.49 ; *P* = 0.003). The average ADC, rCBV and metabolite ratios in low-grade gliomas and non-neoplastic lesions are illustrated in Table 1.

Diagnostic performance of different MRI parameters for differentiation between low-grade gliomas and non-neoplastic lesions

The ROC curve analysis for ADC, rCBV and metabolite ratios between low-grade gliomas and non-neoplastic lesions is shown in Fig. 1. The area under the curve (AUC) of ROC analysis was good for rCBV and Cho/NAA ratios (> 0.80) and fair for Cho/Cr and NAA/Cr ratios (0.70–0.80) in differentiating between low-grade gliomas and non-neoplastic lesions. The sensitivity was highest for rCBV and Cho/NAA ratios, and the specificity was highest for NAA/Cr ratio. When the rCBV measurements were combined with MRS ratios, significant improvement was observed in the AUC (0.969).

Table 1 Average ADC, rCBV and metabolite ratios in low-grade gliomas and non-neoplastic lesions

Group	<i>n</i>	ADC (mean ± SD)	rCBV (mean ± SD)	Cho/Cr (mean ± SD)	Cho/NAA (mean ± SD)	NAA/Cr (mean ± SD)
Low-grade glioma	12	1.13 ± 0.32	1.27 ± 0.45	2.14 ± 0.71	3.34 ± 1.5	0.62 ± 0.3
All non-neoplastic lesions	27	1.2 ± 0.5	0.75 ± 0.22	1.65 ± 1.1	1.5 ± 1.6	1.46 ± 1.5
Tumefactive demyelination	7	0.96 ± 0.14	1 ± 0.2	1.85 ± 0.9	2.2 ± 2	1 ± 0.5
Tuberculoma	4	1.4 ± 0.4	0.8 ± 0.2	1.4 ± 0.33	1.14 ± 0.3	1.3 ± 0.7
Cavernoma	4	1.3 ± 0.5	0.45 ± 0.12	0.78 ± 0.5	0.66 ± 0.33	1.4 ± 1.1
Ischemia	4	0.97 ± 0.6	0.74 ± 0.14	1.1 ± 0.3	0.33 ± 0.2	4.4 ± 2
Encephalitis	3	1.65 ± 0.5	0.83 ± 0.03	1.58 ± 0.3	1.52 ± 0.3	1 ± 0.1
Vasculitis	2	1.65 ± 0.3	0.92 ± 0.2	1.34 ± 0.4	1.5 ± 0.5	0.96 ± 0.1
Pyogenic abscess	2	0.64 ± 0.04	0.49 ± 0.04	3.96 ± 0.76	4.26 ± 1.2	0.67 ± 0.2
Tylor cortical dysplasia	1	1	0.8	1.2	0.61	1.98
<i>P</i> value^a	–	0.74	< 0.001*	0.045*	0.002*	0.003*

The cut of value and the important numbers are also in bold

* Statistically significant

^a *P* value for comparison between low-grade gliomas and all non-neoplastic lesions

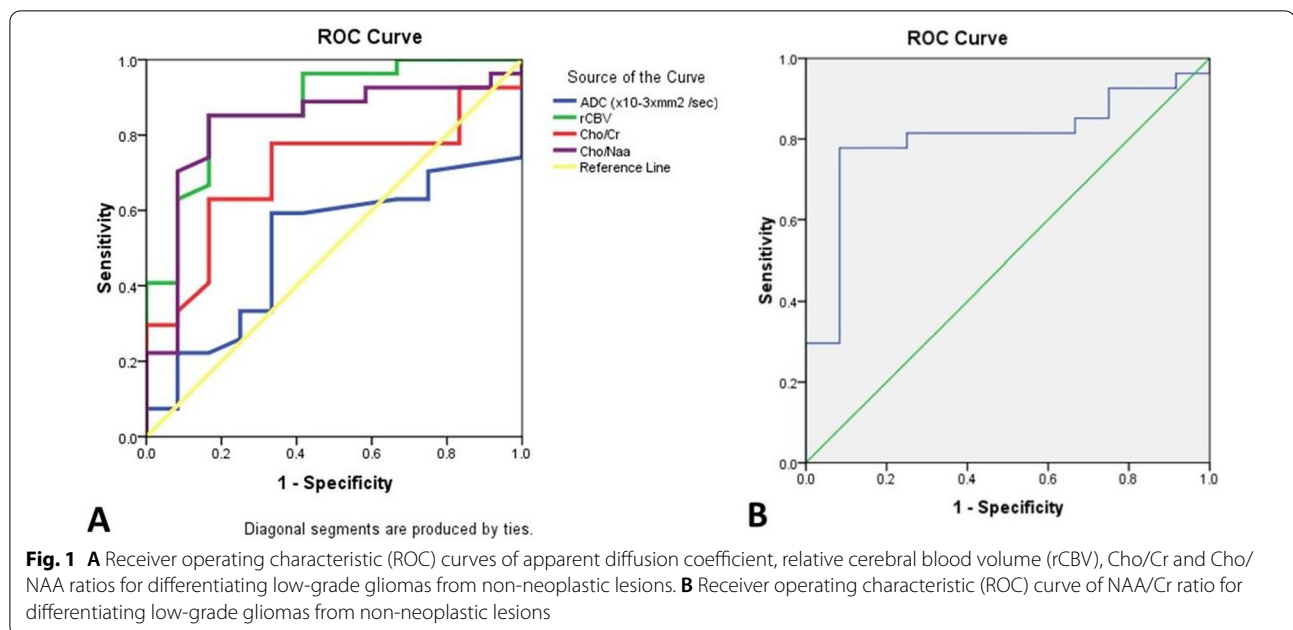


Table 2 Sensitivity, specificity, positive predictive value, negative predictive value, accuracy and confidence intervals for different MRI parameters

Parameter	AUC (95% CI)	Cut off point	Sensitivity%	Specificity%	PPV %	NPV %	Accuracy %
ADC	0.508 (0.321–0.695)	≤ 1.125	59.3	66.7	80.0	42.1	61.5
rCBV	0.875 (0.756–0.994)	≥ 0.93	85.2	83.3	92.0	71.4	84.6
Cho/Cr	0.704 (0.536–0.871)	≥ 1.97	77.8	66.7	84.0	57.1	74.4
Cho/NAA	0.829 (0.682–0.976)	≥ 2.5	85.2	83.3	92.0	71.4	84.6
NAA/Cr	0.799 (0.651–0.948)	≤ 0.79	77.8	91.7	95.5	64.7	82.1

The cut of value and the important numbers are also in bold

with improved diagnostic accuracy (89.7%) and sensitivity (88.9%). Table 2 demonstrates the corresponding sensitivity, specificity, positive predictive value, negative predictive value, accuracy and confidence intervals of different MRI parameters.

Diagnostic performance of rCBV and Cho/NAA ratio for differentiation between low-grade gliomas and non-neoplastic lesions

The ROC analysis demonstrated that a threshold value ≥ 0.93 for rCBV (AUC 0.875, PPV = 92%, NPV = 71.4%) and a threshold value ≥ 2.5 for Cho/NAA (AUC = 0.829, PPV = 92%, NPV = 71.4%) had 85.2% sensitivity and 83.3% specificity for predicting neoplastic lesions (Figs. 2, 3).

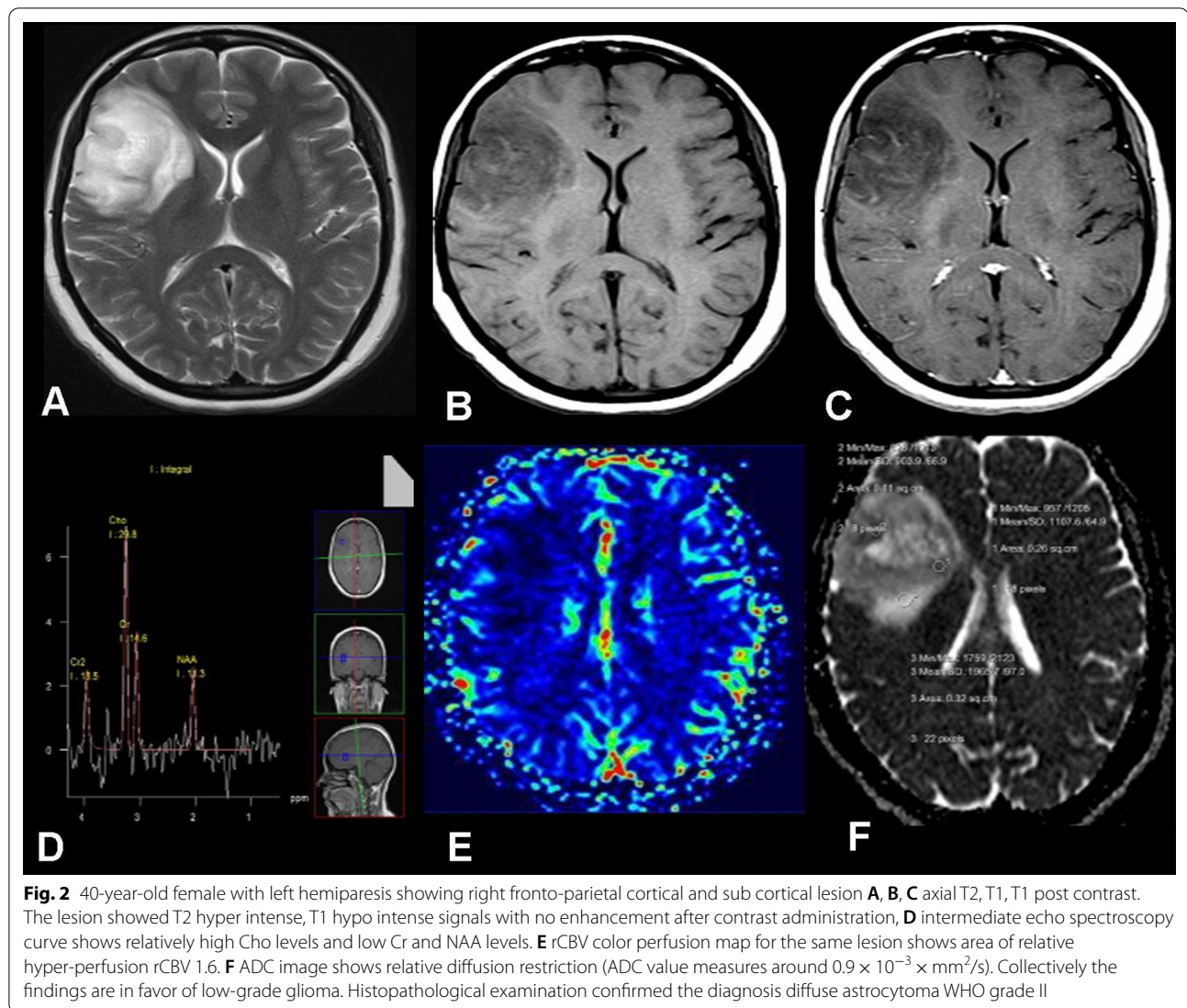
Using rCBV cutoff value of 0.93, two cases of neoplastic lesions were misclassified as non-neoplastic because their rCBV values were less than 0.93. Among non-neoplastic lesions, four cases (3 tumefactive demyelinating lesions,

1 tuberculoma) had rCBV slightly more than 0.93 (1.07–1.18). For Cho/NAA ratio, two neoplastic lesions were misclassified as non-neoplastic as their Cho/NAA ratio was less than 2.5. Four cases of non-neoplastic lesions showed Cho/NAA ratio exceeding 2.5 (pyogenic abscess, $n = 2$ and tumefactive demyelinating lesions, $n = 2$).

Discussion

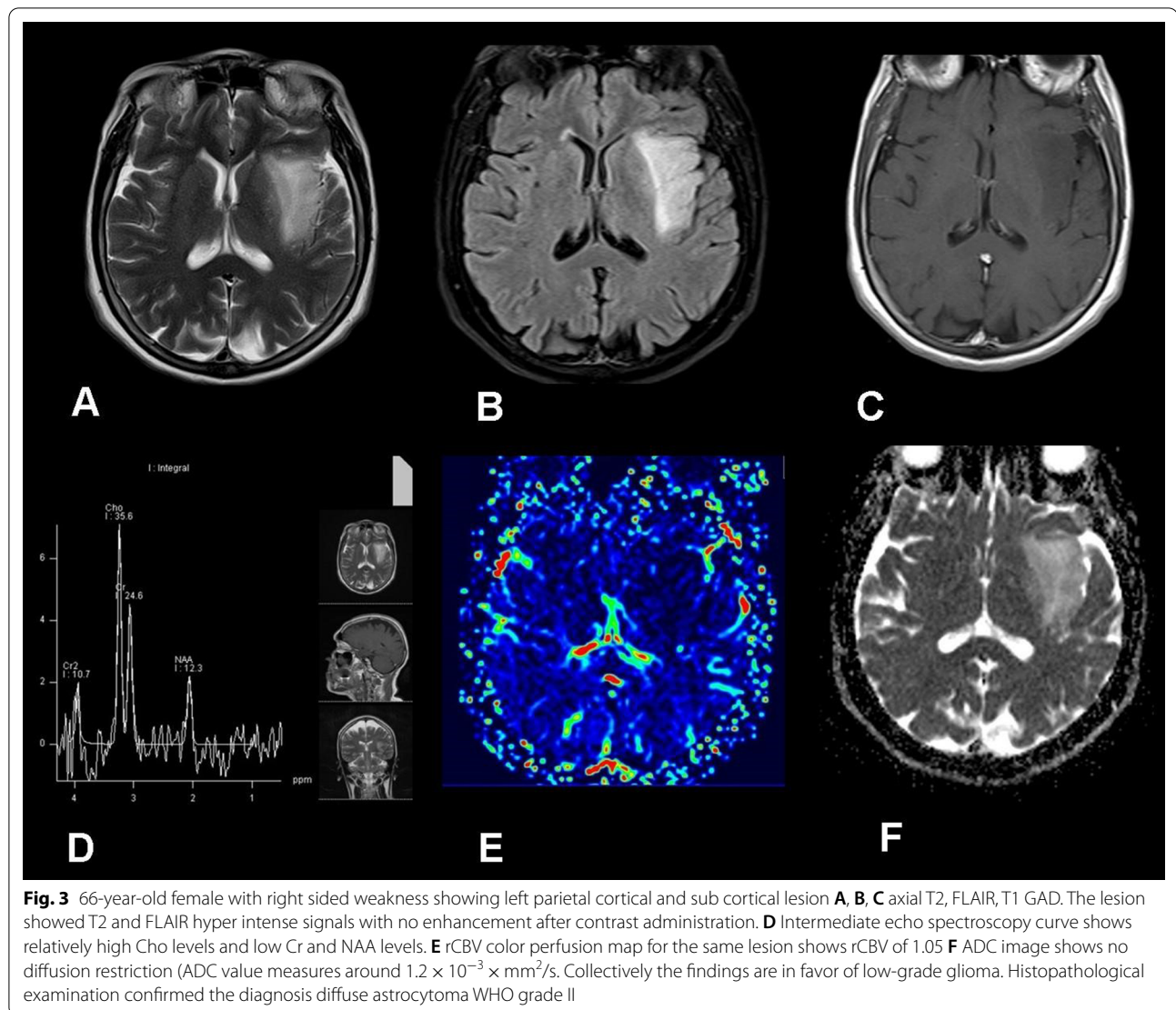
In an attempt to differentiate low-grade glioma and non-neoplastic lesions, our data showed that higher rCBV (≥ 0.93) and higher Cho/NAA (≥ 2.5) values favor a diagnosis of low-grade glioma over non-neoplastic process.

At MR perfusion, mean rCBV for low-grade gliomas in our study was 1.27 ± 0.45 . Our results were similar to Abrigo et al. [16] as they reported that the average rCBV of 83 low-grade gliomas included in their meta-analysis was 1.29. When comparing rCBV among low-grade gliomas and non-neoplastic lesion, we found that rCBV was significantly higher in low-grade gliomas ($P < 0.001$). This



is matching with previous study by Floriano et al. [17] where they reported higher rCBV in low-grade gliomas when compared to non-neoplastic brain lesions, the only difference is that they specifically studied infectious brain lesions. Hourani et al. [18] compared patients with neoplastic brain lesions and non-neoplastic brain lesions (including stroke, demyelinating disease, multiple sclerosis and acute disseminated encephalomyelitis); they found higher mean rCBV values in low-grade tumors (1.45 ± 1.16) in comparison with non-neoplastic lesions (1.0 ± 0.4); however, the difference in their study was not statistically significant ($P = 0.73$). This could be explained by difference in subtypes of low-grade gliomas included in their study were gangliogliomas and oligodendrogliomas were included, in our study only diffuse astrocytoma (WHO grade II) were included.

Tumefactive demyelinating lesions (TDLs) are one of the most common brain lesions to mimic a brain tumor. These lesions are large (> 2 cm) inflammatory lesions that can be associated with edema and mass effect. Multiple sclerosis is considered the most frequent etiology, but the differential diagnosis includes a wide spectrum of diseases, including neuromyelitis optica spectrum disorders and Acute Disseminated Encephalomyelitis [19, 20]. Parks et al. [21] reported that mean rCBV in TDLs was 1.14 ± 0.38 and the maximum rCBV among TDLs was 1.55. In our study, rCBV in TDLs was 1 ± 0.2 ; it was slightly higher than the suggested threshold for differentiating low grade gliomas from non-neoplastic lesions. Herimath et al. [22] in their study, found that the mean rCBV in TDLs was 2.11 ± 1.12 . They suggested that the relatively high rCBV in TDLs could be attributed to angiogenesis and vasodilation in both acute and chronic



demyelinating plaques, which may be the cause of disease progression.

Parenchymal tuberculomas are the most common form of intracranial parenchymal tuberculosis. They can occur in any location in the brain, including basal cisterns, brainstem and cerebral hemispheres. In children, they are more common in infratentorial locations but in adults they are predominantly supratentorial. Intra-axial tuberculomas are difficult to differentiate from primary brain tumors on conventional MRI [23]. Soni et al. [24] in their study, using arterial spin labeling, found that tuberculomas were hypoperfused. On the other hand, Ghosh et al. reported higher rCBV value in tuberculomas (3.36 ± 1.38) [25]. They attributed the high rCBV reported in their study to the presence of innumerable inflammatory cells in the wall of tubercular granuloma which may have elicited a strong

neovascular response [25]. In the current study, rCBV of tuberculomas ranged between 0.056 and 1.07, where only one case showed an rCBV slightly higher than 0.93.

At MRS, we found that Cho/NAA ratio was significantly higher in low-grade gliomas as compared to non-neoplastic lesions (3.34 ± 1.53 vs 1.50 ± 1.60 ; $P=0.002$). Elevated Cho and reduced NAA levels were observed in both groups; however, it is more pronounced in brain tumors. Similar results have been observed by Baloš et al. [26] where Cho/NAA ratio was significantly higher in low-grade gliomas as compared to non-neoplastic lesions in their study (3.60 ± 4.35 vs 0.91 ± 0.49).

Cho is increased in conditions with high cell membrane turnover or higher cell density from tumor proliferation. NAA is a neuronal marker and it decreases when there is pathological replacement of healthy brain tissue. In acute

demyelinating lesions increased Cho and decreased NAA levels can be observed, this may be attributed to inflammation, demyelination, axonal degeneration and reactive gliosis, which may lead to misdiagnosis of these lesions as neoplasms [27]. Increased Cho/Cr ratio was observed in 4 out of 7 cases with TDLs in our study, with increased Cho/NAA and decreased NAA/Cr ratios in two of them, however low rCBV value in these cases helped correct suggestion of non-neoplastic condition which was confirmed by positive response to steroid therapy (Fig. 4).

In patients with pyogenic abscess ($n=2$), lactate and lipid peaks were detected in addition to increase Cho/NAA, Cho/Cr and decreased NAA/Cr ratios mostly due to contamination by surrounding brain tissues, similar to previously published results [28]. These data in addition

to evident diffusion restriction and low rCBV values in both cases the diagnosis of pyogenic abscess was made, which was confirmed at histopathology after surgical intervention. In our study, when the rCBV measurements were combined with MRS ratios, significant improvement was observed in the AUC (0.969) with improved diagnostic accuracy (89.7%) and sensitivity (88.9%) for differentiating low-grade gliomas from mimicking non-neoplastic lesions.

At DWI, ADC measurements can offer quantitative data regarding the restriction of movement of water molecules in tissues [29]. In our series, ADC values in low-grade gliomas and non-neoplastic lesions were not statistically different (1.2 ± 0.5 vs. 1.13 ± 0.32 ; $P=0.74$). Similarly, Baloš et al. [26] in a study included 25 patients

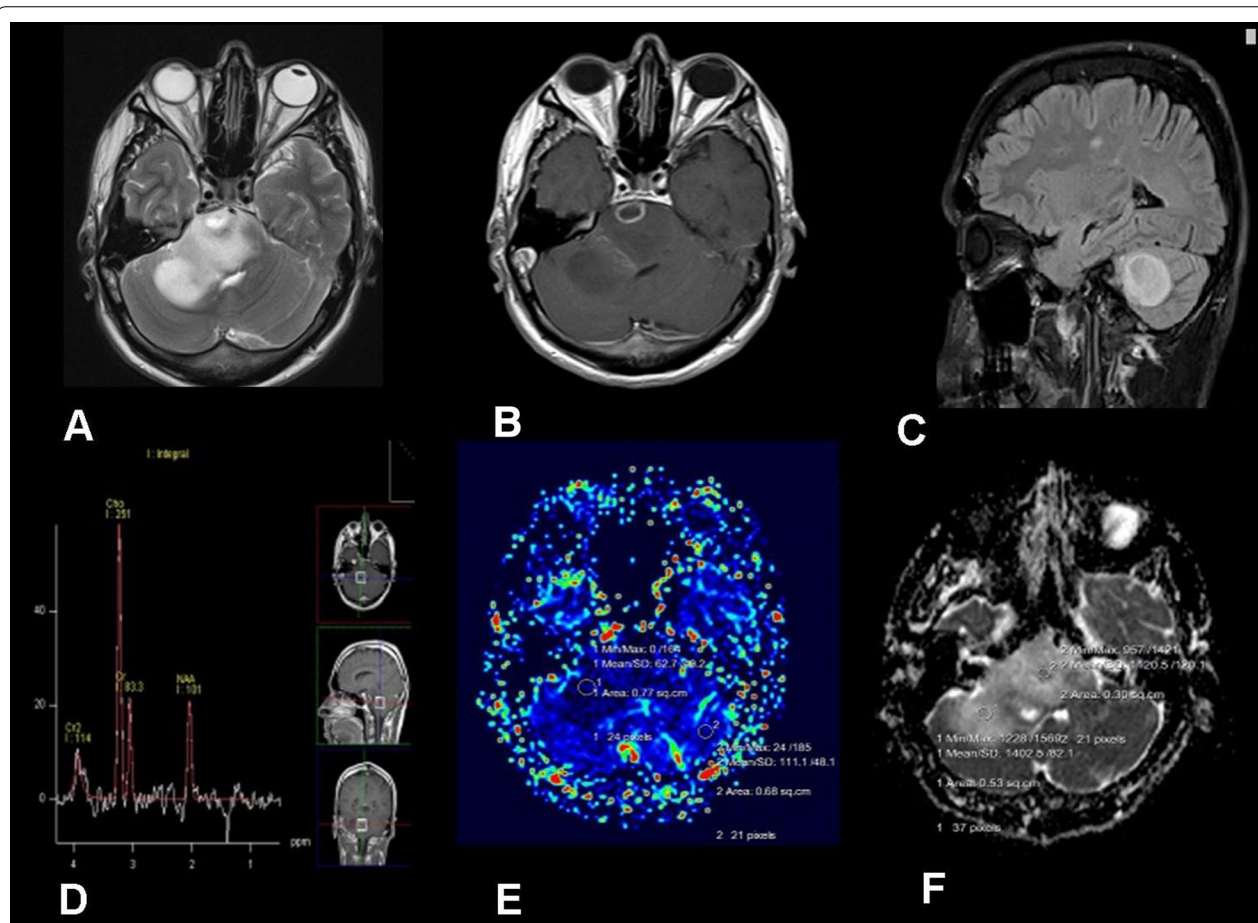


Fig. 4 24-year-old male with blurring of vision. **A, B** Axial T2 and T1 post contrast showed T2 hyper-intense expanding lesion epicentered on the right brachium pontis extending into the pons and the right cerebellar hemisphere with focus of ring enhancement after contrast associated and mild mass effect. **C** Right para sagittal FLAIR image showing hyper intense mass at the right cerebellar hemisphere and multiple other deep and periventricular white matter hyper intense foci. **D** Intermediate echo spectroscopy curve shows high Cho levels and relatively low Cr and NAA levels. **E** rCBV color perfusion map for the same lesion shows area of relative hypo-perfusion (rCBV 0.84). **F** ADC image show Foci of diffusion restrictions at the right brain stem (ADC value measures around $(0.98 \times 10^{-3} \times \text{mm}^2/\text{s})$). Collectively the findings are in favor of tumefactive demyelinating lesion. Post therapy follow up confirmed the diagnosis

with non-neoplastic lesions (including; hamartoma, ischemic and demyelinating lesions) and 14 patients with low-grade gliomas (diffuse astrocytoma, oligoastrocytoma, oligodendroglioma); ADC value was 1.14 ± 0.41 and 1.32 ± 0.42 , respectively, with no significant difference between both groups. Yoon et al. [30] found in their study that DWI enabled to differentiate abscess from other mass like intra-axial brain lesions. The lowest ADC values in our study were found in patients with pyogenic abscess (Fig. 5).

Although the results from our current study are encouraging, there are a few limitations. First, a relatively small number of patients were included in each group and subgroups. Second, we did not have neuropathological confirmation in most of the non-neoplastic lesions; however, this highlights the importance of non-invasive imaging methods in diagnosis of non-neoplastic

pathologies. Third, molecular characterization of low-grade gliomas was not done in our study.

Conclusion

MR diffusion, perfusion and spectroscopy are non-invasive methods that add detailed information about cellularity, vascularity and metabolic composition of mass like intra-axial lesions of the brain. Evaluation of rCBV and metabolite ratios at MRS, particularly Cho/NAA ratio, may be helpful in differentiating low-grade gliomas from non-neoplastic lesions. The combination of DSC perfusion and MRS can significantly improve the diagnostic accuracy and can help avoiding the need for an invasive biopsy.

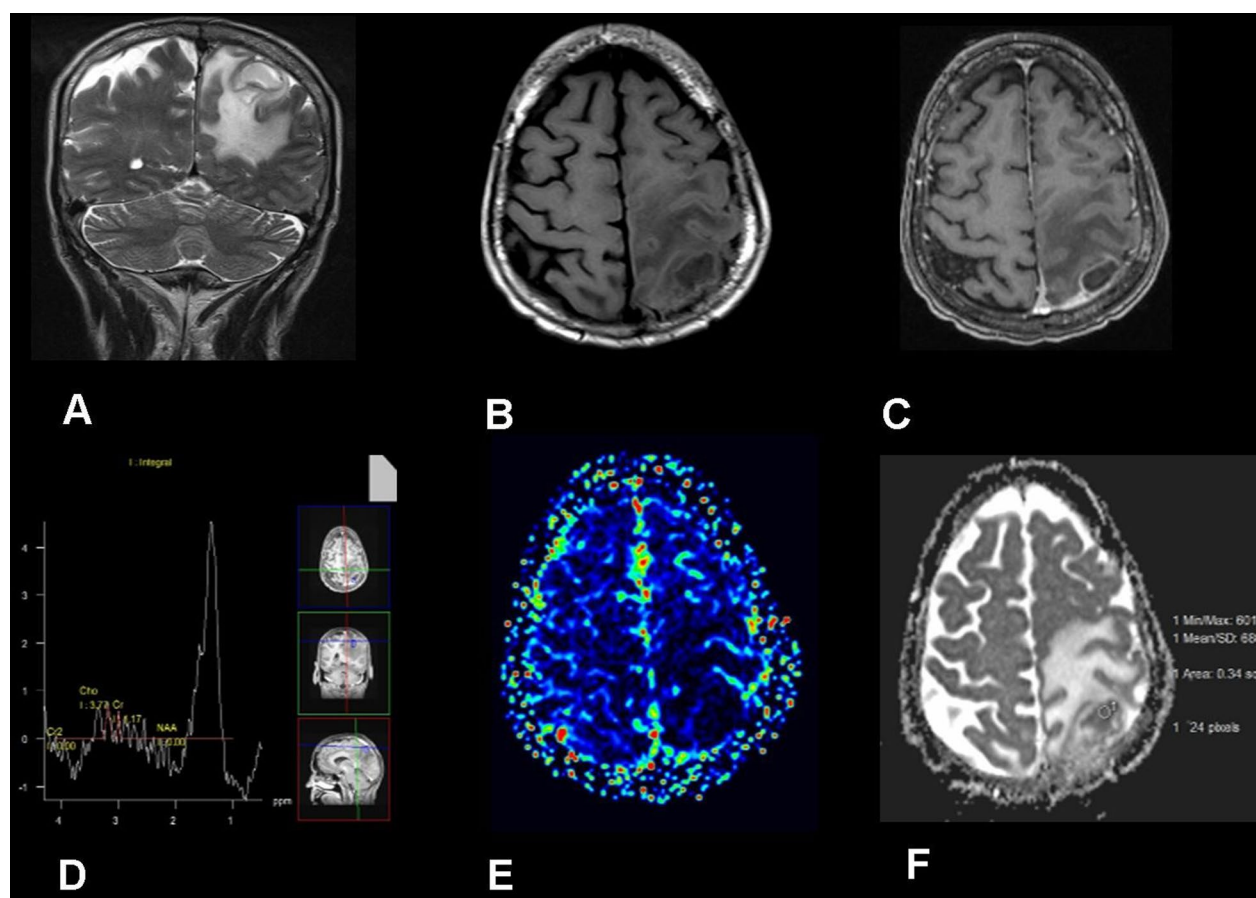


Fig. 5 53-year-old male with severe headache showing left high posterior parietal cystic lesion surrounded by vasogenic edema **A, B, C** coronal T2, axial T1 and T1 GAD. The lesions show T2 hyper intense core and hypo intense thin rim, T1 hypo intense core and iso intense rim with intense peripheral rim and related meningeal enhancement after contrast administration. **D** Intermediate echo spectroscopy curve shows relatively depleted Cho, Cr and NAA levels with very high lipid peaks at (0.9–1.3 ppm). **E** rCBV color perfusion map for the same lesion shows area of relative hypo-perfusion (rCBV = 0.4). **F** ADC image shows evident diffusion restriction (ADC value measures around $0.68 \times 10^{-3} \times \text{mm}^2/\text{s}$, collectively the findings are in favor of pyogenic cerebral abscess. Post-operative data confirmed the diagnosis

Abbreviations

CSI: Chemical shift imaging; DSC: Dynamic susceptibility contrast; DWI: Diffusion weighted images; rCBV: Relative cerebral blood volume; ROC: Receiver operating characteristic; NAA: *N*-Acetyl aspartate; Cho: Choline; Cr: Creatine; PPV: Positive predictive value; NPV: Negative predictive value; AUC: Area under the curve; TDL: Tumefactive demyelinating lesion.

Acknowledgements

Not applicable.

Authors' contributions

MSA Carried out cases on workstation and selection of research cases, prepare the figures for cases demonstration, writing and review of the research. MHK: writing the research, selection of the cases; figures preparation of cases. MISR carried out cases on workstation and selection of research cases. EA carried the pathological analysis of the biopsies. AHF clinical assessment of cases and carried the biopsy specimens "All authors read and approved the final manuscript". NE writing the research, selection of the cases; figures preparation of cases. All authors read and approved the final manuscript.

Funding

This study had no funding from any resource.

Availability of data and materials

The datasets used and/or analyzed during the current study are available from the corresponding author on reasonable request.

Declarations

Ethics approval and consent to participate

All procedures followed were in accordance with the ethical standards of the responsible committee on human experimentation (Institutional Review Board (IRB) of Faculty of Medicine Alexandria University and with the Helsinki Declaration of 1964 and later versions. Committee's reference number is unavailable (NOT applicable). Consents were obtained from the patients for the study.

Consent for publication

All patients included in this research gave written informed consent to publish the data contained within this study.

Competing interests

The authors declare that they have no competing interests.

Author details

¹Radiology Department, National Liver Institute, Menoufia University, Shibin Al Kawm, Egypt. ²Radiology Department, Faculty of Medicine, Alexandria University, Alexandria, Egypt. ³Pathology Department, Faculty of Medicine, Alexandria University, Alexandria, Egypt. ⁴Neurosurgery Department, Faculty of Medicine, Alexandria University, Alexandria, Egypt.

Received: 13 August 2021 Accepted: 30 December 2021

Published online: 07 January 2022

References

- Young GS (2007) Advanced MRI of adult brain tumors. *Neurol Clin* 25(4):947–973
- Al-Okaili RN, Krejza J, Woo JH (2007) Intra-axial brain masses: MR imaging-based diagnostic strategy—initial experience. *Radiology* 243:539–550
- Henson JW, Gonzalez RG (2004) Neuroimaging in glioma therapy. *Expert Rev Neurother* 4(4):665–671
- Barker PB, Bizzi A, De Stefano N, Gullapalli R, Lin DDM (2010) Clinical MR spectroscopy: techniques and applications. Cambridge University Press, New York, pp 1–212
- Tate AR, Underwood J, Acosta D, Julia-Sape M, Majos C, Mroeno-Torres A et al (2006) Development of a decision support system for diagnosis and grading of brain tumors using in vivo magnetic resonance single voxel spectra. *NMR Biomed* 19:411–434
- Fan GG, Deng QL, Wu ZH, Guo QY (2006) Usefulness of diffusion/perfusion-weighted MRI in patients with non-enhancing supratentorial brain gliomas: a valuable tool to predict tumor grading? *BJR* 79:652–658
- Helenius J, Soine L, Perkiö J, Salonen O, Kangasmäki A, Kaste M et al (2002) Diffusion-weighted MR imaging in normal human brains in various age groups. *AJNR Am J Neuroradiol* 23(2):194–199
- Schaefer PW, Grant PE, Gonzalez RG (2000) Diffusion-weighted MR imaging of the brain. *Radiology* 217:331–345
- Edelenyi FS, Rubin C, Esteve F, Grand S, Decorps M, Lefournier V et al (2000) A new approach for analyzing proton magnetic resonance spectroscopic images of brain tumors: nosologic images. *Nat Med* 6:1287–1289
- Chavhan GB, Babyn PS, Thomas B, Shroff MM, Haacke EM (2009) Principles, techniques, and applications of T2*-based MR imaging and its special applications. *Radiographics* 29(5):1433–1449
- Van der Graaf M (2009) In vivo magnetic resonance spectroscopy: basic methodology and clinical applications. *Eur Biophys J* 10:517–530
- Posse S, Otazo R, Tsai SY, Yoshimoto AE, Lin FH (2009) Single-shot MR spectroscopic imaging with partial parallel imaging. *Magn Reson Med* 61(3):541–547
- Moseley ME, Liu C, Rodriguez S, Brosnan T (2009) Advances in magnetic resonance neuroimaging. *Neurol Clin* 27(1):1–19
- Ginsberg LE, Fuller GN, Hashmi M (1998) The significance of lack of MR contrast enhancement of supratentorial brain tumors in adults: histopathological evaluation of a series. *Surg Neurol* 49(4):436–440
- Mechtler L (2008) Neuroimaging in neuro-oncology. *Neurol Clin* 27:171–201
- Abrigo JM, Fountain DM, Provenzale JM, Law EK, Kwong JS, Hart MG, Tam WWS (2018) Magnetic resonance perfusion for differentiating low-grade from high-grade gliomas at first presentation. *Cochrane Database Syst Rev* 1(1):CD011551
- Florianio VH, Torres US, Spotti AR, Ferraz-Filho JR, Tognola WA (2013) The role of dynamic susceptibility contrast-enhanced perfusion MR imaging in differentiating between infectious and neoplastic focal brain lesions: results from a cohort of 100 consecutive patients. *PLoS ONE* 8(12):e81509
- Hourani R, Brant LJ, Rizk T, Weingart JD, Barker PB, Horska A (2008) Can proton MR spectroscopic and perfusion imaging differentiate between neoplastic and non-neoplastic brain lesions in adults. *AJNR* 29:366–372
- Mabray MC, Cohen B, Villanueva-Meyer J, Valles F, Barajas R, Rubenstein J (2015) Performance of apparent diffusion coefficient values and conventional MRI features in differentiating tumefactive demyelinating lesions from primary brain neoplasms. *AJR Am J Roentgenol* 205:1075–1085
- Suh CH, Kim HS, Jung SC, Choi CG, Kim SJ (2018) MRI findings in tumefactive demyelinating lesions: a systematic review and meta-analysis. *AJNR Am J Neuroradiol* 39(9):1643–1649
- Parks NE, Bhan V, Shankar J (2016) Perfusion imaging of tumefactive demyelinating lesions compared to high grade gliomas. *Can J Neurol Sci* 43(2):316–318
- Hiremath SB, Muraleedharan A, Kumar S, Nagesh C, Kesavadas XC, Abraham XM et al (2017) Combining diffusion tensor metrics and DSC perfusion imaging: can it improve the diagnostic accuracy in differentiating tumefactive demyelination from high-grade glioma? *AJNR Am J Neuroradiol* 38:685–690
- Khatri GD, Krishnan V, Antil N, Saigal G (2018) Magnetic resonance imaging spectrum of intracranial tubercular lesions: one disease, many faces. *Pol J Radiol* 29(83):e524–e535
- Soni N, Srindharan K, Kumar S, Mishra P, Bathla G, Kalita J, Behari S (2018) Arterial spin labeling perfusion: prospective MR imaging in differentiating neoplastic from non-neoplastic intra-axial brain lesions. *Neuroradiol J* 31(6):544–553
- Ghosh RN, Vyas S, Singh P, Khandelwal N, Sankhyani N, Singhi P (2019) Perfusion magnetic resonance imaging in differentiation of neurocysticercosis and tuberculoma. *Neuroradiology* 61(3):257–263
- Balos DR, Gavrilović S, Lavrić S, Vasić B, Macvanski M, Damjanović D et al (2013) proton magnetic resonance spectroscopy and apparent diffusion coefficient in evaluation of solid brain lesions. *Vojnosanit Pregl* 70(7):637–644
- Brandão LA, Castillo M (2016) Adult brain tumors: clinical applications of magnetic resonance spectroscopy. *Magn Reson Imaging Clin N Am* 24(4):781–809
- Elshafey R, Hassanein A, Shakal A, Mokbel E (2014) H proton MR spectroscopy and diffusion-weighted imaging in discrimination between

pyogenic brain abscesses and necrotic brain tumors. *Egypt J Radiol Nucl Med* 45:889–896

29. Yao R, Cheng A, Liu M, Zhang Z, Jin B, Yu H (2021) The diagnostic value of apparent diffusion coefficient and proton magnetic resonance spectroscopy in the grading of pediatric gliomas. *J Comput Assist Tomogr* 45(2):269–276
30. Yoon RG, Kim HS, Hong GS, Park JE, Jung SC, Kim SJ et al (2018) Joint approach of diffusion- and perfusion-weighted MRI in intra-axial mass like lesions in clinical practice simulation. *PLoS ONE* 13(9):e0202891

Publisher's Note

Springer Nature remains neutral with regard to jurisdictional claims in published maps and institutional affiliations.

Submit your manuscript to a SpringerOpen[®] journal and benefit from:

- Convenient online submission
- Rigorous peer review
- Open access: articles freely available online
- High visibility within the field
- Retaining the copyright to your article

Submit your next manuscript at ► [springeropen.com](https://www.springeropen.com)
